



University of Groningen

## Recombination-Limited Photocurrents in Low Bandgap Polymer/Fullerene Solar Cells

Lenes, Martijn; Morana, Mauro; Brabec, Christoph J.; Blom, Paul W. M.

*Published in:*  
Advanced Functional Materials

*DOI:*  
[10.1002/adfm.200801514](https://doi.org/10.1002/adfm.200801514)

**IMPORTANT NOTE:** You are advised to consult the publisher's version (publisher's PDF) if you wish to cite from it. Please check the document version below.

*Document Version*  
Publisher's PDF, also known as Version of record

*Publication date:*  
2009

[Link to publication in University of Groningen/UMCG research database](#)

### *Citation for published version (APA):*

Lenes, M., Morana, M., Brabec, C. J., & Blom, P. W. M. (2009). Recombination-Limited Photocurrents in Low Bandgap Polymer/Fullerene Solar Cells. *Advanced Functional Materials*, 19(7), 1106-1111. <https://doi.org/10.1002/adfm.200801514>

### **Copyright**

Other than for strictly personal use, it is not permitted to download or to forward/distribute the text or part of it without the consent of the author(s) and/or copyright holder(s), unless the work is under an open content license (like Creative Commons).

### **Take-down policy**

If you believe that this document breaches copyright please contact us providing details, and we will remove access to the work immediately and investigate your claim.

*Downloaded from the University of Groningen/UMCG research database (Pure): <http://www.rug.nl/research/portal>. For technical reasons the number of authors shown on this cover page is limited to 10 maximum.*

# Recombination-Limited Photocurrents in Low Bandgap Polymer/Fullerene Solar Cells

By Martijn Lenes, Mauro Morana, Christoph J. Brabec, and Paul W. M. Blom\*

The charge transport and photogeneration in solar cells based on the low bandgap-conjugated polymer, poly[2,6-(4,4-bis-(2-ethylhexyl)-4H-cyclopenta[2,1-b; 3,4-b']dithiophene)-alt-4,7-(2,1,3-benzothiadiazole)] (PCPDTBT) and fullerenes is studied. The efficiency of the solar cells is limited by a relatively low fill factor, which contradicts the observed good and balanced charge transport in these blends. Intensity dependent measurements display a recombination limited photocurrent, characterized by a square root dependence on effective applied voltage, a linear dependence on light intensity and a constant saturation voltage. Numerical simulations show that the origin of the recombination limited photocurrent stems from the short lifetime of the bound electron-hole pairs at the donor/acceptor interface.

## 1. Introduction

Conjugated polymers blended with soluble fullerene derivatives show a great potential for low cost, large area photovoltaics.<sup>[1]</sup> One of the main problems in these polymer/fullerene bulk heterojunction (BHJ) solar cells is the poor overlap between the solar spectrum and the absorption of the materials used. In order to increase the photon harvesting smaller bandgap polymers are needed. One route toward expanding the absorption toward higher wavelengths is by coupling electron donor and acceptor units together in a polymer. Most of the polymers created using this route; however, have resulted in significantly inferior performances compared to solar cells based on poly(3-hexylthiophene) (P3HT). The main reason for the low performance is mainly due to the poor carrier transport in these polymers, resulting in low fill factors and quantum efficiencies.<sup>[2–9]</sup> One of the most promising devices following this approach are based on poly [2,6-(4,4-bis-(2-ethylhexyl)-4H-cyclopenta[2,1-b; 3,4-b']dithiophene)-alt-4,7-(2,1,3-benzothiadiazole)] (PCPDTBT), reaching power conversion efficiencies of up to 3.2% when combined with [6,6]-phenyl-C<sub>71</sub>-butyric acid methyl ester

(PC<sub>70</sub>BM).<sup>[10]</sup> In spite of the increased absorption the power efficiency is still lower than the state-of-the-art P3HT/fullerene cells, of which efficiencies have been reported of more than 5%.<sup>[11]</sup> The efficiency is mainly limited by a low fill factor (FF) of only 40%. In earlier investigations it has been demonstrated that a strongly unbalanced charge transport leads to space charge limited photocurrents, characterized by a square root dependence on applied voltage.<sup>[12]</sup> This dependence limits the fill factor to about 40%. Remarkably, measurements performed on PCPDTBT-based field effect transistors resulted in hole mobilities in the polymer as high as  $2 \times 10^{-6} \text{ m}^2 \text{ V}^{-1} \text{ s}^{-1}$ .<sup>[10]</sup>

Even though field-effect mobilities are quantitatively difficult to relate to charge carrier mobilities in actual solar cells, due to the much lower charge carrier densities in the latter devices,<sup>[13]</sup> the high field-effect mobilities clearly indicate that the quality of the hole transport in PCPDTBT must be very good.<sup>[14]</sup> Combined with the electron transport properties of intrinsic PCBM films, which already have been investigated in great detail,<sup>[15]</sup> a balanced transport is therefore expected. Consequently, the origin of the reduced fill factors and external quantum efficiencies in these blends is not clear. In this study the charge transport and photogeneration of PCPDTBT/PCBM solar cells is studied to gain more insight into the loss mechanisms in these type of devices.

## 2. Results and Discussion

### 2.1. Charge Transport in Pristine PCPDTBT Films

As mentioned above, even though field-effect mobilities give a valuable insight into the quality of the charge carrier transport, ideally one would like to measure the charge carrier mobility in a similar device geometry as the actual solar cell. Here, the charge transport is studied in a vertical device geometry similar to solar cells. By choosing suitable top and bottom contacts (see Section 4) one can either inject both charge carriers, or choose to block one carrier and measure either the hole or electron current.<sup>[16]</sup> The transport through these single carrier devices is modeled with a space charge limited current (SCLC) using a field dependent mobility.<sup>[17]</sup> Figure 1 shows the measured *J*–*V* characteristics of a

[\*] Prof. P. W. M. Blom, M. Lenes  
Molecular Electronics, Zernike Institute for Advanced Materials  
Nijenborgh 4, 9747 AG Groningen (The Netherlands)  
E-mail: p.w.m.blom@rug.nl  
Dr. M. Morana, Dr. C. J. Brabec  
Konarka Austria  
Altenbergerstrasse 69, 4040 Linz (Austria)

DOI: 10.1002/adfm.200801514

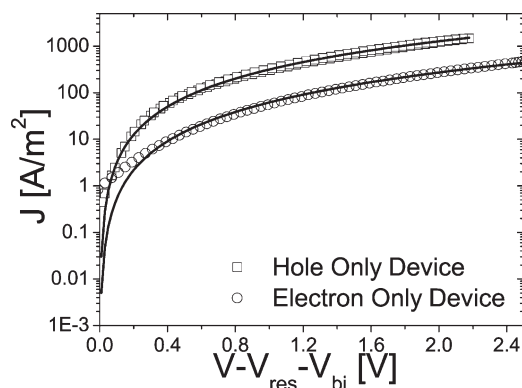


**Figure 1.**  $J$ - $V$  characteristics, corrected for built in voltage and series resistance, of a PCPDTBT hole and electron only device. Data is fitted (solid line) with a space charge limited current using a field dependent mobility resulting in a hole mobility of  $5.5 \times 10^{-8} \text{ m}^2 \text{ Vs}^{-1}$  and electron mobility of  $4 \times 10^{-9} \text{ m}^2 \text{ Vs}^{-1}$ .

hole only device of PCPDTBT. From the  $J$ - $V$  measurements we determine the zero-field mobility to be  $5.5 \times 10^{-8} \text{ m}^2 \text{ Vs}^{-1}$ . This mobility is about a factor of 30 lower than the earlier reported field-effect mobility,<sup>[10]</sup> similar differences between FET and diode mobilities have been observed in P3HT due to the density dependence of the mobility.<sup>[13]</sup> However, the observed SCL hole mobility of  $5.5 \times 10^{-8} \text{ m}^2 \text{ Vs}^{-1}$  for PCPDTBT is about a factor of 2–3 larger than the mobility obtained in SCL diodes based on pristine regio-regular P3HT.<sup>[18]</sup> As a result in its pristine form PCPDTBT is at least as good as a hole transporter as regio-regular P3HT.

Since the electron transport in polymer/fullerene blends occurs through the fullerene phase, electron transport through the polymer is of no importance for the device operation of organic solar cells. Nevertheless, we also studied the electron transport through pristine PCPDTBT films also shown in Figure 1. As reported previously,<sup>[10]</sup> the polymer also shows signs of electron transport. In fact, the observed electron mobility of  $4 \times 10^{-9} \text{ m}^2 \text{ Vs}^{-1}$  is only one order of magnitude lower than the hole mobility. Interestingly, the electron transport in the pristine material can be fitted by a model combining SCLC type transport in combination with a field dependent mobility.<sup>[17]</sup>

## 2.2. Charge Transport in PCPDTBT/PCBM Blends

Blending a polymer with a fullerene often significantly alters the charge carrier transport in both polymer and fullerene compared to the pristine case. For instance, in the case of MDMO-PPV, a 200-fold increase in hole mobility is observed when blending the polymer with PCBM.<sup>[18]</sup> On the other side, blending P3HT with PCBM results in a reduced hole transport, only to be recovered by thermal or solvent annealing.<sup>[19,20]</sup> Therefore, single carrier measurements on the actual blend used in the solar cell are needed to relate the charge carrier transport to the solar cell performance. Blends of PCPDTBT and PCBM were prepared in a 1 to 4 weight ratio which was reported to be optimal.<sup>[10]</sup> The charge transport is determined in single carrier devices as

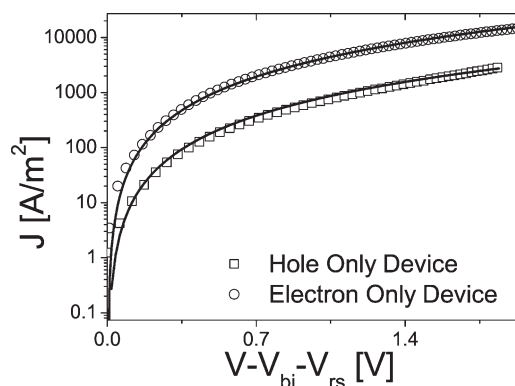


**Figure 2.**  $J$ - $V$  characteristics, corrected for built in voltage and series resistance, of a PCPDTBT/PCBM hole and electron only device. Data is fitted with a space charge limited current using a field dependent mobility resulting in a hole mobility in the blend of  $3 \times 10^{-8} \text{ m}^2 \text{ Vs}^{-1}$  and an electron mobility of  $7 \times 10^{-8} \text{ m}^2 \text{ Vs}^{-1}$ .

described above for pristine polymer films. Figure 2 shows the  $J$ - $V$  characteristic of a hole and electron only device of a PCPDTBT/PCBM blend. The determined hole mobility of PCPDTBT in the blend of  $3 \times 10^{-8} \text{ m}^2 \text{ Vs}^{-1}$  almost equals the hole mobility in pristine films. This indicates that the hole transport in the polymer is not altered by blending it with PCBM. Furthermore, the determined hole mobility is equal to hole mobilities reported in MDMO-PPV/PCBM (1:4) blends<sup>[16]</sup> and P3HT/PCBM (1:1) blends after annealing.<sup>[18]</sup> The determined electron mobility of  $7 \times 10^{-8} \text{ m}^2 \text{ Vs}^{-1}$  is slightly lower than values reported for MDMO-PPV/PCBM and P3HT/PCBM blends, that typically amount to  $1.0 \times 10^{-7}$ – $2.0 \times 10^{-7} \text{ m}^2 \text{ Vs}^{-1}$ .<sup>[18–20]</sup> Similar electron and hole mobility values were found by ambipolar transport studies on OFETs at high fullerene loadings.<sup>[21]</sup>

The single carrier measurements presented here demonstrate that in the blends the hole and electron mobilities are balanced and closely match the mobilities reported for MDMO-PPV and P3HT based blends. It is therefore, highly unlikely that the relatively low quantum efficiencies and fill factors are a consequence of unbalanced transport or too low charge carrier mobilities and more investigation of the solar cells is needed.

## 2.3. PCPDTBT/PCBM Solar Cells

The inset of Figure 3 shows the current versus voltage ( $J$ - $V$ ) curve at room temperature of a typical PCPDTBT/PCBM solar cell made in this study. The external quantum efficiency (see Fig. 4) has been determined at ECN in Petten to estimate the correct short circuit current under AM 1.5 illumination and thus the mismatch factor of our measurements. Efficiencies of 2.2% are obtained which is somewhat lower than the 2.7% reported previously for PCPDTBT/PC61BM.<sup>[10]</sup> As reported previously the power conversion efficiency is limited by a low external quantum efficiency (<35%) and fill factor (40%). For studying the device physics it is very useful to plot the photocurrent of a solar cell as a function of effective applied voltage. The photocurrent is defined as  $J_{\text{ph}} = J_{\text{L}} - J_{\text{D}}$ , where  $J_{\text{L}}$  and  $J_{\text{D}}$  are the current density under

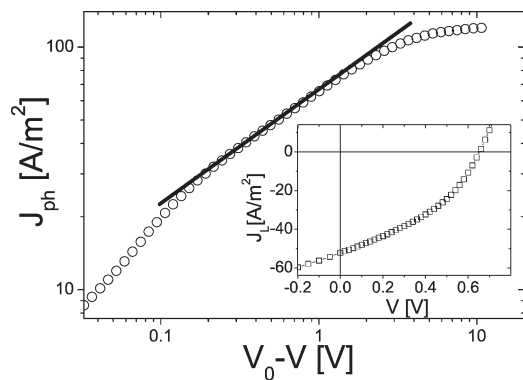


**Figure 3.** Photocurrent of a PCPDTBT/PCBM solar cell versus effective applied voltage under illumination of a AM1.5 simulated solar spectrum from a Steuernagel SolarConstant 1200 light source with a light output equivalent to an AM1.5 light source intensity of  $0.7 \text{ kW m}^{-2}$ . The black line indicates a square root dependence. Inset:  $J$ - $V$  characteristics of a PCPDTBT/PCBM solar cell.

illumination and in dark, respectively, and the effective applied voltage as  $V_{\text{eff}} = V_0 - V_A$ . Here,  $V_0$  is the compensation voltage defined as  $J_{\text{ph}}(V_0) = 0$  and  $V_A$  is the applied bias. The photocurrent versus effective applied voltage of a PCPDTBT/PCBM solar cell is also shown in Figure 3. It is clear that at large reverse bias the photocurrent saturates, at which point all the generated electron-hole pairs are dissociated and collected at the electrodes, which indicates that the mean electron and hole drift lengths  $w_{e(h)} = \mu_{e(h)} \tau_{e(h)} E$  are equal to, or larger than the sample thickness  $L$  and no recombination occurs.<sup>[22]</sup> The photocurrent shows a sharp decrease at lower effective applied voltages, resulting in a rather low short circuit current and low fill factor. Furthermore, a square root dependence of the photocurrent as a function of effective voltage is observed, as is indicated by the black line. The origin of such a square root dependence of the photocurrent has been explained by Goodman and Rose in 1971.<sup>[22]</sup> If the mean electron or hole (or both) drift length becomes smaller than  $L$ , recombination of charge carriers becomes considerable. If there is also a difference between hole and electron drift length, a non-uniform electric field will occur across the devices, which will give rise to a square root dependent

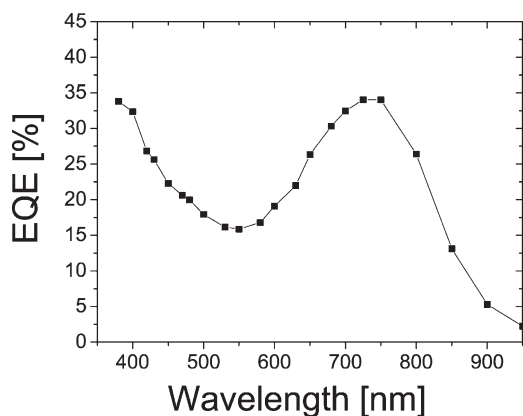


**Figure 4.** External quantum efficiency of a PCPDTBT/PCBM solar cell.

photocurrent:

$$J_{\text{ph}} = qG \sqrt{\mu_{h(e)} \tau_{h(e)}} \sqrt{V} \quad (1)$$

with  $G$  the generation rate of free charge carriers. Here, a low mobility or short lifetime of the free carriers, due to recombination or trapping, limits the photocurrent. Additionally, at high light intensities the build up of space charges (which is the origin of the non-uniform electric field) reaches a fundamental limit. In this limit the maximum electrostatically allowed photocurrent is limited by the mobility of the slowest charge carrier and is given by

$$J_{\text{ph}} \leq (qG)^{0.75} \left( \frac{9}{8} \epsilon_0 \epsilon_r \mu_h \right)^{0.25} \sqrt{V} \quad (2)$$

which again has a square root dependence on voltage. The latter has been experimentally demonstrated in a system where the charge carrier mobilities are heavily unbalanced.<sup>[12]</sup> The way to distinguish between these two physically distinct cases is by light intensity dependent measurements. Where in the first (recombination limited) case the photocurrent scales linearly with light intensity, in the second (the space-charge limited) case it scales with a three-fourth power law dependence. Furthermore, the point at which the square root regime forms a transition into the saturation regime, the saturation voltage  $V_{\text{sat}}$ , is either independent on light intensity (recombination-limited) or scales with a one half power on light intensity (space-charge limited case). From Figure 5 it is clear that with decreasing light-intensity  $V_{\text{sat}}$  is not changing, as expected for a recombination-limited photocurrent. Furthermore, in Figure 6 it is shown that in the square root regime the photocurrent is linearly scaling with light intensity. As a result the photocurrent observed for PCPDTBT/PCBM devices clearly shows the fingerprints of a recombination-limited photocurrent. Since, the mobilities of the charge carriers in the device are known we can estimate the lifetime using Equation (1), resulting in a lifetime of  $\sim 10^{-7}$ . This value,

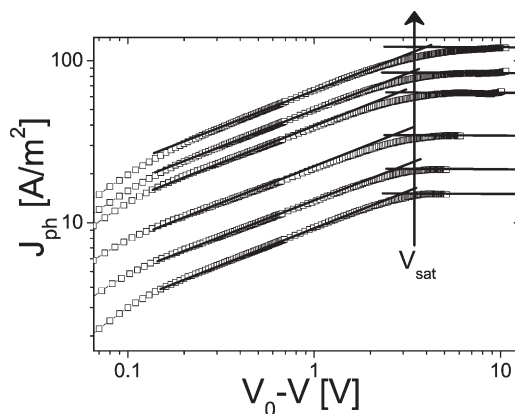


**Figure 5.** Photocurrent of a PCPDTBT/PCBM solar cell versus effective applied voltage at different intensities. Solid lines indicate square root and saturation regimes as a guide for the eye where  $V_{\text{sat}}$  indicates the saturation voltage.

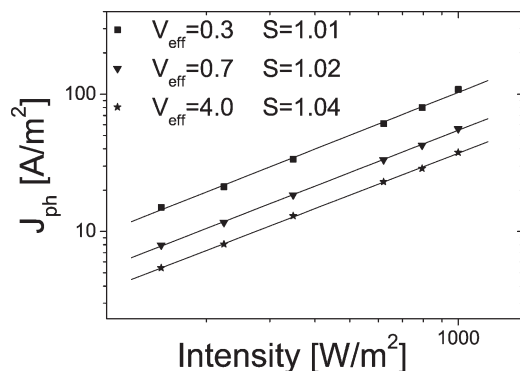


**Figure 6.** Intensity dependence of the photocurrent at different effective voltages. The slope ( $S$ ), determined from the linear fit (solid lines) to the experimental data is indicated in the figure.

estimated under the assumption that the dominant limitation comes from the hole transport, may slightly change if electron transport is considered as well.

## 2.4. Device Simulations and Discussion

In a polymer/fullerene solar cell the photogenerated excitons dissociate at the donor-acceptor interface via an ultrafast electron transfer from the donor to the acceptor. However, the ultrafast electron transfer to the acceptor does not directly result in free carriers, but in a bound electron-hole pair (due to the Coulomb attraction between the carriers). This pair also needs to be dissociated, assisted by temperature and by the internal electric field, before it decays to the ground state.<sup>[20]</sup> As proposed by Braun, this bound pair is metastable, enabling multiple dissociations and being revived by the recombination of free charge carriers via Langevin recombination.<sup>[23]</sup> Finally, the free carriers are transported to the electrodes, a process governed by charge carrier mobility. In the above mentioned Goodman and Rose model a direct generation of free carriers (from now on called  $G_{GR}$ ) is assumed. In a polymer/fullerene solar cell; however, the amount of generated free carriers will not only depend on the amount of generated bound electron-hole pairs ( $G_B$ ), but also on their dissociation probability ( $P$ ). In that case the generation rate of bound pairs  $G_B$  is proportional to the incident light intensity and is taken as a measure for the amount of absorbed photons (assuming that all generated excitons dissociate at the donor/acceptor interface). As a result, when Equation 1 is applied to an organic solar cell the calculated lifetime can only be considered as an effective lifetime ( $\tau_{eff}$ ). This can be seen more clearly when one considers the device at open circuit voltage: since no charges are extracted ( $J_{ph} = 0$ ) there is an equilibrium between the generation and recombination of free charge carriers in the device, given by:

$$G_{GR} = \frac{n}{\tau_{eff}} \quad (3)$$

with  $n=p$  being the free carrier density and  $G_{GR}$  the recombination rate of free carriers. Thus, if  $\tau_{eff}$  is small, indicating lots of recombination, also the free carrier density will be small for a given generation rate of free carriers  $G_{GR}$ . When the formation and dissociation of bound electron-hole pairs as an intermediate step is taken into account the amount of free carriers that are generated will be given by  $PG_B$  and hence one can state that

$$PG_B = \frac{n}{\tau} \quad (4)$$

where  $\tau$  is now the true lifetime of free charge carriers as given by Langevin recombination.

One can also say that

$$G_B = \frac{n}{P\tau} = \frac{n}{\tau_{eff}} \quad (5)$$

Thus, when the bound-pair generation rate  $G_B$  is taken as a measure for the amount of generated charges, as has been done in device modeling, the effective lifetime  $\tau_{eff}$  can be small either due to a small life-time  $\tau$  of the free carriers or due to a low dissociation probability  $P$  of the bound pairs.

In order to disentangle the effects of  $P$  and  $\tau$  on  $\tau_{eff}$  we performed device simulations using a numerical program which solves Poisson's equation and the continuity equations, including diffusion, bimolecular recombination (Langevin type, governed by the slowest charge carrier),<sup>[24]</sup> space-charge effects and charge dissociation of bound electron-hole pairs.<sup>[25]</sup> Relevant parameters for the simulation program are the charge carrier mobilities, including their field and/or density dependence, dielectric constant  $\epsilon$ , separation distance  $a$  and the decay rate of bound electron-hole pair  $k_f$ . Since the charge carrier mobilities are measured and the dielectric constant is known only  $a$  and  $k_f$  are used as fitting parameters. Figure 7 shows the fit of the simulation program using  $a = 2.1 \times 10^{-9}$  m and  $k_f = 1.7 \times 10^7$  s<sup>-1</sup>. Using the same fit parameters we can fit all measured light intensities. When the calculated dissociation probability is compared with the measured and simulated photocurrent (as is indicated

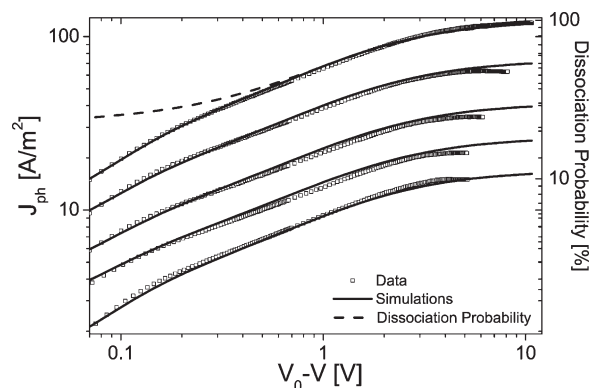


**Figure 7.** Simulation of the photocurrent at different intensities. Symbols represent measurement, solid line fit to the data, dotted line calculated dissociation efficiency.



in Fig. 7) it is clear that the strong field dependence of the photocurrent for effective voltages  $>0.4$  V originates from the field dependent dissociation of the bound electron-hole pairs. What is striking in the device simulations is the high value of  $k_f$  needed to fit the data. As an indication, for MDMO-PPV/PCBM and P3HT/PCBM cells a value of  $\sim 10^4$  is found. This indicates that the solar cells are limited by a high decay-rate, and thus short lifetime, of the bound electron-hole pair. Recently, Hwang *et al.* have shown experimental evidence of such an intermediate charge transfer state with a short lifetime using photoinduced absorption spectra.<sup>[26]</sup> To indicate the strong effect this decay rate has on the performance of the solar cells, simulations with a decrease in  $k_f$  have been performed up to the point at which the decay rate is equal to P3HT and MDMO-PPV values (see Fig. 8). Upon lowering of the decay rate the typical square root behavior disappears and the photocurrent becomes significantly less field dependent, manifesting itself in a greatly increased short circuit current and fill factor. The simulations indicate that when  $k_f$  for the PCPDTBT/PCBM devices would be as low as for the P3HT/PCBM cells an efficiency of  $\sim 7\%$  can be achieved. This demonstrates the potential of these low band gap polymer/fullerene devices, when the increased recombination of the bound pairs can be prevented.

Above, we have shown that PCPDTBT/PCBM solar cells show signs of a recombination limited photocurrent as predicted by Goodman and Rose. Using our numerical simulation program we are able to show that the low dissociation probability is the cause of the low lifetime of the free carriers  $\tau_{\text{eff}}$ . We show the lifetime of the bound electron-hole pair to be significantly shorter compared to other polymer/fullerene systems. Moreover, the effective lifetime predicted using Equation (1)  $\sim 10^{-7}$  s $^{-1}$ , matches the lifetime of the bound pair  $1/k_f$  ( $k_f = 1.7 \times 10^7$  s $^{-1}$ ) predicted by the simulation model.

Therefore, we can conclude that the decrease of the photocurrent at low effective voltages, and hence low fill factor of the device, is due to a short lifetime of the bound electron-hole pairs. In earlier work an almost complete intermixing of the

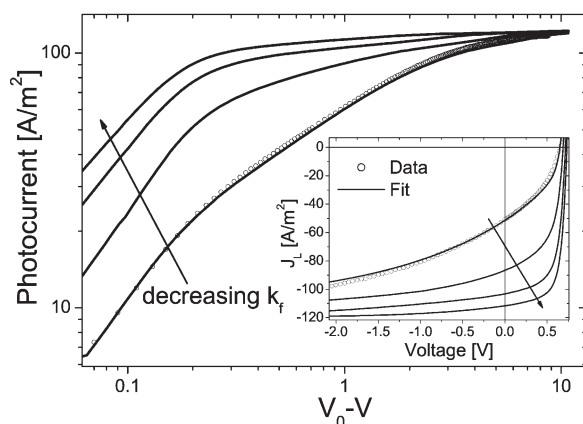


**Figure 8.** Simulation of photocurrent for different values of the decay rate  $k_f$  starting from the determined decay rate of  $1.7 \times 10^7$  s $^{-1}$  and decreasing one order at a time until the value of  $1.7 \times 10^4$  s $^{-1}$  typical for normal polymer/fullerene systems. Inset: Simulation of the current under illumination for these values of  $k_f$ .

PCPDTBT polymer with PCBM at the molecular level was reported.<sup>[27]</sup> When donor and acceptor are too closely intermixed carriers can end up being trapped in dead ends and will not dissociate fully into free carriers leading to a large decay rate and hence small effective lifetime. Unfortunately, changing solvent, deposition procedures, and using annealing effects do not result in a more phase separated morphology.<sup>[21]</sup> However, recent results on PCPDTBT/PCBM solar cells by Peet *et al.* have shown that the addition of alkanedithiols to the solution results in a dramatic increase in device performance.<sup>[28]</sup> It is shown that adding alkanedithiol results in larger phase separation of donor and acceptor which in turn results in a much higher fill factor and external quantum efficiency. Apparently, the larger phase separation results in an increase of the effective lifetime of the charge carriers, such that the device is no longer recombination limited, as predicted by the simulations. Furthermore, transient absorption spectroscopy performed on blends with and without dithiol show a significant decrease in geminate recombination for the latter which is in agreement with our results.<sup>[29]</sup>

### 3. Conclusions

The charge transport and photogeneration in PCPDTBT/PCBM solar cells is studied to gain insight into the loss mechanisms in these devices. The hole transport in the polymer phase has been shown to be unaffected upon blending with fullerenes, with a mobility of  $5.5 \times 10^{-8}$  m $^2$  Vs $^{-1}$ . The electron mobility of PCBM in the blend has been determined to be  $7 \times 10^{-8}$  m $^2$  Vs $^{-1}$ , which is slightly lower than the pristine value for PCBM. Thus, the electron and hole transport are almost balanced and the mobilities are sufficiently high to reach high fill factors and efficiencies. Nevertheless, the fill factor of PCPDTBT/PCBM solar cells is relatively low, originating from a square root regime in the photocurrent as a function of effective voltage. The photocurrent has shown to be recombination limited, characterized by a square root dependence on effective applied voltage, a linear dependence on light intensity and a constant saturation voltage. Simulations of the photocurrent show that the solar cells are limited by a short lifetime of bound electron hole pairs. We suggest that, this short lifetime is due to an unfavorable morphology where donor and acceptor are too intimately mixed.

### 4. Experimental

For the hole-only devices and solar cells prepatterned ITO-covered glass substrates were first cleaned using soap water, acetone, demineralized water, propanol and an UV-ozone treatment. Subsequently, a layer of PEDOT/PSS (Bayer AG) was spin-coated under ambient conditions onto the cleaned substrates and the layer was dried by annealing the substrate. After spincoating either the pristine polymer or the polymer/fullerene blend from chloroform resulting in a layer thickness of  $\sim 120$  nm the devices were completed by thermal evaporation of a 5 nm samarium/100 nm aluminum (solar cells) or 20 nm palladium/80 nm gold (hole only devices) top contact under vacuum ( $5 \times 10^{-6}$  mbar, 1 ppm O $_2$  and  $<1$  ppm H $_2$ O). For the electron only devices a 30 nm aluminum layer is deposited on glass by thermal evaporation followed by spincoating either the pristine polymer or the polymer blend from chloroform and thermal evaporation of a 5 nm samarium/100 nm aluminum top contact. The current density versus voltage curves were measured in a N $_2$  atmosphere at room temperature

using a computer controlled Keithley 2400 Source Meter.  $J$ - $V$  characteristics of the solar cells were performed under illumination of an AM1.5 simulated solar spectrum from a Steuernagel SolarConstant 1200 light source with a light output equivalent to an AM1.5 light source intensity of  $0.7\text{ kW m}^{-2}$ . A set of neutral density filters is used for the intensity dependence measurements. EQE measurements performed at ECN were done using a white light halogen lamp in combination with a series of interference filters.

## Acknowledgements

The work of M. L. forms part of the research program of the Dutch Polymer Institute (project no. 524). The Authors would like to acknowledge S. C. Veenstra at ECN for the external quantum efficiency measurements.

Received: October 10, 2008

Revised: December 9, 2008

Published online: February 26, 2009

- [1] C. J. Brabec, N. S. Sariciftci, J. C. Hummelen, *Adv. Funct. Mater.* **2001**, *11*, 15.
- [2] S. E. Shaheen, D. Vangeneugden, R. Kiebooms, D. Vanderzande, T. Fromherz, F. Padinger, C. J. Brabec, N. S. Sariciftci, *Synth. Met.* **2001**, *121*, 1583.
- [3] C. Winder, G. Matt, J. C. Hummelen, R. A. J. Janssen, N. S. Sariciftci, C. J. Brabec, *Thin Solid Films* **2002**, *403–404*, 373.
- [4] A. Dhanabalan, J. K. J. van Duren, P. A. van Hal, J. L. J. van Dongen, R. A. J. Janssen, *Adv. Funct. Mater.* **2001**, *11*, 255.
- [5] A. P. Smith, R. R. Smith, B. E. Taylor, M. F. Durstock, *Chem. Mater.* **2004**, *16*, 4687.
- [6] X. Wang, E. Perzon, F. Oswald, F. Langa, S. Admassie, M. R. Andersson, O. Inganäs, *Adv. Funct. Mater.* **2005**, *15*, 1665.
- [7] X. Wang, E. Perzon, J. L. Delgado, P. de la Cruz, F. Zhang, F. Langa, M. Andersson, O. Inganäs, *Appl. Phys. Lett.* **2004**, *85*, 5081.
- [8] F. Zhang, E. Perzon, X. Wang, W. Mammo, M. R. Andersson, O. Inganäs, *Adv. Funct. Mater.* **2005**, *15*, 745.
- [9] L. M. Campos, A. Tontcheva, S. Günes, G. Sonmez, H. Neugebauer, N. S. Sariciftci, F. Wudl, *Chem. Mater.* **2005**, *17*, 4031.
- [10] D. Mühlbacher, M. Scharber, M. Morana, Z. Zhu, D. Waller, R. Gaudiana, C. Brabec, *Adv. Mater.* **2006**, *18*, 2884.
- [11] M. D. Irwin, D. B. Buchholz, A. W. Hains, R. P. H. Chang, T. J. Marks, *PNAS* **2008**, *8*, 2783.
- [12] V. D. Mihailetchi, J. Wildeman, P. W. M. Blom, *Phys. Rev. Lett.* **2005**, *94*, 126602.
- [13] C. Tanase, E. J. Meijer, P. W. M. Blom, D. M. de Leeuw, *Phys. Rev. Lett.* **2003**, *91*, 216601.
- [14] M. Morana, P. Koers, C. Waldauf, M. Koppe, D. Muehlbacher, P. Denk, M. Scharber, D. Waller, C. Brabec, *Adv. Funct. Mater.* **2007**, *17*, 3274.
- [15] V. D. Mihailetchi, J. K. J. van Duren, P. W. M. Blom, J. C. Hummelen, R. A. J. Janssen, J. M. Kroon, M. T. Rispens, W. J. H. Verhees, M. M. Wienk, *Adv. Funct. Mater.* **2003**, *13*, 43.
- [16] V. D. Mihailetchi, L. J. A. Koster, P. W. M. Blom, C. Melzer, B. de Boer, J. K. J. van Duren, R. A. J. Janssen, *Adv. Funct. Mater.* **2005**, *15*, 795.
- [17] P. N. Murgatroyd, *J. Phys. D* **1970**, *3*, 151.
- [18] V. D. Mihailetchi, H. Xie, B. de Boer, L. J. A. Koster, P. W. M. Blom, *Adv. Funct. Mater.* **2006**, *16*, 699.
- [19] V. D. Mihailetchi, H. Xie, L. J. A. Koster, B. de Boer, L. M. Popescu, J. C. Hummelen, P. W. M. Blom, *Appl. Phys. Lett.* **2006**, *89*, 012107.
- [20] V. D. Mihailetchi, L. J. Koster, J. C. Hummelen, P. W. Blom, *Phys. Rev. Lett.* **2004**, *93*, 216601.
- [21] M. Morana, M. Wegscheider, A. Bonanni, N. Kopidakis, S. Shaheen, M. Scharber, Z. Zhu, D. Waller, R. Gaudiana, C. J. Brabec, *Adv. Funct. Mat.* **2008**, *18*, 1757.
- [22] A. M. Goodman, A. Rose, *J. Appl. Phys.* **1971**, *42*, 2823.
- [23] C. L. Braun, *J. Chem. Phys.* **1984**, *80*, 4157.
- [24] L. J. A. Koster, V. D. Mihailetchi, P. W. M. Blom, *Appl. Phys. Lett.* **2006**, *88*, 052104.
- [25] L. J. A. Koster, E. C. P. Smits, V. D. Mihailetchi, P. W. M. Blom, *Phys. Rev. B* **2005**, *72*, 085205.
- [26] I. W. Hwang, C. Soci, D. Moses, Z. Zhu, D. Waller, R. Gaudiana, C. J. Brabec, A. J. Heeger, *Adv. Mater.* **2007**, *19*, 2307.
- [27] Z. Zhu, D. Waller, R. Gaudiana, M. Morana, D. Mühlbacher, M. Scharber, C. J. Brabec, *Macromolecules* **2007**, *40*, 1981.
- [28] J. Peet, J. Y. Kim, N. E. Coates, W. L. Ma, D. Moses, A. J. Heeger, G. C. Bazan, *Nat. Mater.* **2007**, *6*, 497.
- [29] T. Clarke, A. Ballantyne, F. Jamieson, C. Brabec, J. Nelson, J. Durrant, *Chem. Comm.* **2009**, *1*, 89.